Superconductivity in the doped $t-J$ model: Results for four-leg cylinders

Hong-Chen Jiang, Zheng-Yu Weng, and Steven A. Kivelson

Phys. Rev. B **98**, 140505 — Published 19 October 2018

DOI: 10.1103/PhysRevB.98.140505

Superconductivity in the doped t-J model: results for four-leg cylinders

Hong-Chen Jiang,[1,*] Zheng-Yu Weng,[2] and Steven A. Kivelson[3]

[1]*Stanford Institute for Materials and Energy Sciences, SLAC and Stanford University, Menlo Park, California 94025, USA*
[2]*Institute for Advanced Study, Tsinghua University, Beijing, China*
[3]*Physics Department, Stanford University, Stanford, CA, 94305, USA*

(Dated: October 1, 2018)

We report a density-matrix renormalization group study of the lightly doped t-J model on a 4-leg cylinder with doped hole concentrations per site $\delta = 5\% \sim 12.5\%$. By keeping an unusually large number of states and long system sizes, we are able to accurately document the interplay between superconductivity, spin and charge-density-wave orders. The long-distance behavior is consistent with that of a Luther-Emery liquid with a spin-gap and power-law charge-density-wave and superconducting correlations. This is the widest t-J or Hubbard system in which power-law superconducting correlations have been established.

The Hubbard model, and the closely related t-J model, play central roles in the theory of highly correlated electronic systems.[1–18] Enormous effort has been devoted to studying the properties of these models at intermediate couplings. No general theoretically controlled methods exist for this class of problem.[19,20] However, it is possible to obtain essentially exact results on long but moderately narrow cylinders using density matrix renormalization group (DMRG) method.[21] Cylinders have the local lattice geometry of the two-dimensional (2D) system, and can be extrapolated to infinite length, *i.e.* the thermodynamic limit can be taken in one direction. Thus, one can hope to obtain insight into the nature of the 2D problem from these solutions.

In this paper, we report extensive DMRG studies of the 4-leg t-J cylinder, keeping a large number of states so that subtle long-distance correlations can be reliably studied. In addition to the hope that they may shed light on the 2D problem, there are two other reasons to engage in such studies. Firstly, there is interesting physics of multicomponent one-dimensional (1D) systems that can be directly explored without undue speculation - the only extrapolations are to the limits of zero truncation error and infinite system length. Secondly, these systems can be used to benchmark less clearly justified but more widely applicable computational methods.

Principal Findings: We have studied the equal-time superconducting (SC), charge-density-wave (CDW) and spin-density-wave (SDW) correlations for a range of doped hole concentrations, $\delta = 5\% \sim 12.5\%$, and for a characteristic value of $t/J = 3$. We have obtained similar, but less extensive results for other values of t/J. Thought of as a 1D system, we find that the ground-state is always in a Luther-Emery (LE) phase[22] characterized by a finite spin-gap, exponential decay of spin correlations, and CDW and SC correlations that fall at long distances as $\cos(Qr+\theta)\, r^{-K_c}$ and $r^{-K_{sc}}$ respectively, where the CDW wave-vector $Q = 4\pi\delta$. An ordered state with this value of Q has wave-length $\lambda = 1/2\delta$, and so half a doped hole per unit cell corresponding to what is referred to as "half-filled" stripes. This is consistent with recent study of t-t'-U Hubbard model on 4-leg cylinders.[23]

Moreover, within numerical uncertainty, as theoretically expected of a LE liquid, $K_c K_{sc} = 1$ (Fig.3) and the central charge, c, extracted from the scaling of the entanglement entropy, is $c = 1$ (inset of Fig.6). The SC and CDW correlations are invariant with respect to the C_4 symmetry of rotations about the axis of the cylinder. The SC correlations have a "d-wave-like" form factor in that the sign of the pair-field is opposite on bonds perpendicular to and along the cylinder (Y-directed and X-directed bonds). However, this is not a statement of symmetry, and indeed there is an almost equal in strength admixture of an "extended s-wave" component with the consequence that the pair-field amplitude on Y-bonds is two orders of magnitude larger than on X-bonds. (See Fig.2)

For all the dopings studied, $K_{sc} < 2$ and $K_c < 2$, which (assuming the usual emergent Lorentz invariance) implies that both the corresponding susceptibilities diverge as $T \to 0$, as $T^{-(2-K_{sc})}$ and $T^{-(2-K_c)}$ respectively. As far as we know, this is the first demonstration of power-law SC correlations on such a wide t-J or Hubbard cylinder. As shown in Fig.3, K_{sc} is an increasing function of δ and K_c a decreasing function, so that the SC susceptibility is more divergent for $\delta < 0.1$ and the CDW is more divergent for $\delta > 0.1$.

In a previous study[16], we explored the same model over a wider range of parameters in which the primary focus was to explore the extent to which the nature of the ground-state depends on "microscopic details." For the special case on which we focus here, these earlier results are generally consistent with our present results. However, the longer system sizes and the larger number of states used in the present study increase our ability to distinguish exponential-decay correlations, power-law (quasi-long-range) and true long-range order. In particular, what was previously tentatively identified as SC with a long but finite correlation length, we now identify as quasi-long-ranged SC order, albeit with exactly the previously determined form factor.

Model and Method: We study the hole-doped t-J

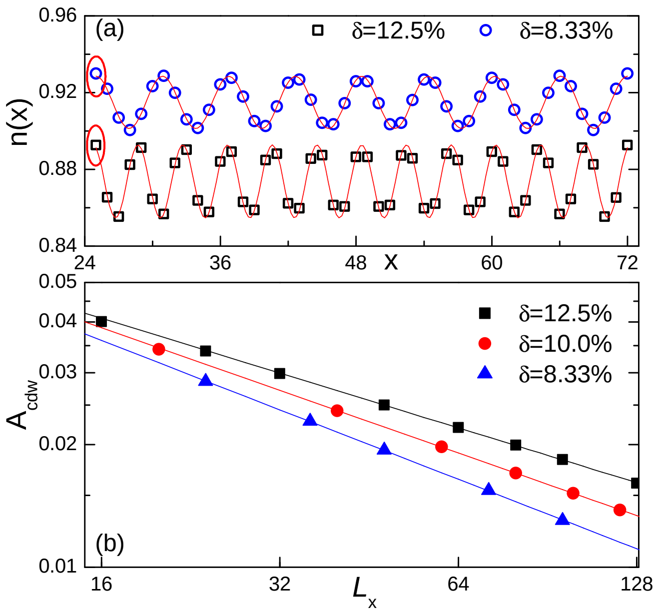

FIG. 1: (Color online) (a) Charge density profile $n(x)$ at doping levels $\delta = 8.33\%$ and $\delta = 12.5\%$ on a $L_x = 96$ cylinder. The open squares and circles denote numerical data, while the red lines are fits to $n(x) = A_{cdw}\cos(Qx+\theta)+n_0$, where A_{cdw} and Q are the CDW amplitude and ordering wave-vector, respectively. Note that only the central-half region with rung indices $\frac{L_x}{4} < x \leq \frac{3L_x}{4}$ are shown and used in the fitting to minimize the boundary effect. The red ovals label the "reference site" chosen to calculate the SC correlation in Eq.(3). (b) Finite-size scaling of A_{cdw} as a function of L_x and δ in a double-logarithmic plot.

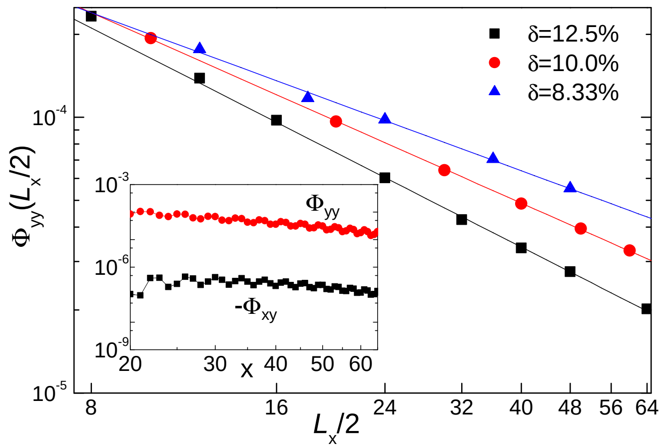

FIG. 2: (Color online) Finite-size scaling of superconducting correlation $\Phi_{yy}(\frac{L_x}{2})$ as a function of L_x and doping level δ in a double-logarithmic plot. The solid lines are fits to $\Phi_{yy}(\frac{L_x}{2}) \sim (\frac{L_x}{2})^{-K_{sc}}$. Inset: Φ_{yy} and -Φ_{xy} on a $L_x = 128$ cylinder.

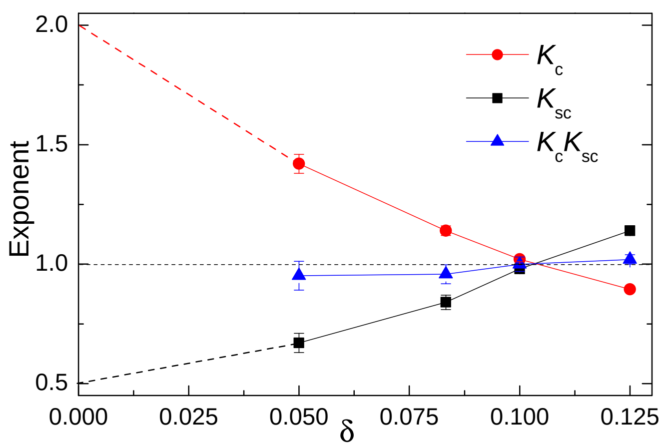

FIG. 3: (Color online) Luttinger exponents K_c, K_{sc} and their product K_cK_{sc}, as a function of δ. The filled symbols represent the extracted values from the fits in Fig.1(b) and Fig.2. The lines are guides to eyes.

model on the square lattice defined by the Hamiltonian

$$H = -t\sum_{\langle ij\rangle\sigma}\left(\hat{c}^+_{i\sigma}\hat{c}_{j\sigma}+h.c.\right) + J\sum_{\langle ij\rangle}\left(\vec{S}_i\cdot\vec{S}_j - \frac{\hat{n}_i\hat{n}_j}{4}\right), \quad (1)$$

where $\hat{c}^+_{i\sigma}$ ($\hat{c}_{i\sigma}$) is the electron creation (annihilation) operator on site $i = (x_i, y_i)$ with spin σ, $\vec{S}_i$ is the spin operator and $\hat{n}_i = \sum_\sigma \hat{c}^+_{i\sigma}\hat{c}_{i\sigma}$ is the electron number operator, $\langle ij\rangle$ denotes nearest-neighbor (NN) sites and the Hilbert space is constrained by the no-double occupancy condition $\hat{n}_i \leq 1$. The parameters t and J are the electron hopping integral and the spin superexchange interactions between NN sites. We take the lattice geometry to be cylindrical and a lattice spacing of unity. Thus, unless stated otherwise, we take periodic boundary conditions in the $\hat{y} = (0,1)$ direction and open in the $\hat{x} = (1,0)$ direction, although for comparison we also consider the case of anti-periodic boundary conditions corresponding to a half-quantum of flux threaded along the cylinder. Here, we focus on cylinders with circumference $L_y = 4$ and length L_x. There are $N = L_x \times L_y$ lattice sites and $N_e \leq N$ electrons. The concentration of "doped holes" is defined as $\delta = \frac{N_h}{N}$, where $N_h = N - N_e$.

For the present study, we focus on the lightly doped case at doping levels $\delta = 5\% \sim 12.5\%$ on cylinders with length up to $L_x = 128$. We set $J = 1$ as the energy unit and report results for $t = 3$. We keep the total magnetization fixed at zero and perform around 60 sweeps and keep up to $m = 15000$ states in each DMRG block with a typical truncation error $\epsilon \lesssim 1\times10^{-7}$. This leads to excellent convergence for our results when extrapolated to $m = \infty$ limit. In all cases, but especially when computing SC correlations, it proves essential to keep very large m and to analyze the $m \to \infty$ seriously, and in some cases, it is necessary to go to system sizes much longer than $L_x = 48$ in order to observe the correlations that arise in the $L_x \to \infty$ limit. Further numerical details are presented in the Supplemental Material[32].

Theoretical expectations: In a LE liquid phase, there is a single gapless spinless bosonic mode with linear dispersion (emergent Lorentz symmetry) - *i.e.* it is asymptotically equivalent to a 1+1 dimensional conformal field theory (CFT) with $c = 1$. At long-distances the density-density correlation oscillates with a well-defined wave-vector Q and decays with a power-law given by the Luttinger exponent K_c, while the dual SC correlation exhibits non-oscillatory power-law decay with exponent $K_{sc} = 1/K_c$. Because there is a spin-gap, spin correlations fall exponentially with a finite correlation length ξ_s, but one can still identify a wave-vector Q_{sdw} which characterizes the oscillations of the SDW correlations.

These properties can be extracted in various ways from numerical data. Because the CDW is pinned by the cylinder ends, an effective method to study the CDW correlations is to compute the charge density modulations in the middle region of a finite cylinder, $\langle \hat{n}_i \rangle \approx (1-\delta) + A_{cdw}(L_x)\cos(Qx_i + \theta)$ for x_i near $L_x/2$. The SC correlation is determined from the long distance behavior of the SC correlator $\Phi_{\alpha,\beta}(x)$ defined in Eq.(3). The expectation is that the decay of these quantities is governed by the appropriate exponents,

$$A_{cdw}(L_x) \propto L_x^{-K_c/2} \text{ and } \Phi_{\alpha\beta}(x) \propto |x|^{-K_{sc}}, \tag{2}$$

where the second relation applies for displacements along the cylinder $1 \ll |x| \ll L_x$. Similarly, Q_{sdw} and ξ_{sdw} can be extracted from the long-distance behavior of the spin-spin correlation.

CDW correlations: To describe the charge density properties of the system, we define the local rung density operator as $\hat{n}(x) = \frac{1}{L_y}\sum_{y=1}^{L_y} \hat{n}(x,y)$ and its expectation value as $n(x) = \langle \hat{n}(x) \rangle$. Fig.1 shows $n(x)$ in a central portion of cylinders with $L_x = 96$ for $\delta = 8.33\%$ and $\delta = 12.5\%$. Here, a stripe pattern with wavelength $\lambda = 1/2\delta$ is found, *i.e.* $\lambda = 4$ for $\delta = 12.5\%$, consistent with previous studies.[16,24]. Similar behavior (not shown) is found at other doping levels. Fig.1(b) shows examples of finite-size scaling of A_{cdw} as a function of L_x. In the double-logarithmic plot, our results for all doping levels are approximately linear, which suggests that $A_{cdw}(L_x)$ decays with a power-law and vanishes as $L_x \to \infty$. The exponent K_c, which is shown in Fig.3, was obtained by fitting the data points using Eq.(2). K_c can also be obtained directly from the decay of the density-density correlation near the cylinder ends (see Supplemental Material[32]).

Superconducting correlation: Since the ground state of the system with even an number of doped holes is always found to have spin 0, we will focus on spin-singlet pairing. A diagnostic of SC order is the pair-field correlator defined as

$$\Phi_{\alpha\beta}(x) = \frac{1}{L_y}\sum_{y=1}^{L_y} \langle \Delta_\alpha^\dagger(x_0,y)\Delta_\beta(x_0+x,y)\rangle. \tag{3}$$

Here the spin-singlet pair-field creation operator is $\Delta_\alpha^\dagger(x,y) = \frac{1}{\sqrt{2}}[c^\dagger_{(x,y),\uparrow}c^\dagger_{(x,y)+\alpha,\downarrow} - c^\dagger_{(x,y),\downarrow}c^\dagger_{(x,y)+\alpha,\uparrow}]$, where bond orientations are designated $\alpha = \hat{x}$, $\hat{y}$, (x_0, y) is the reference bond indicated by the red oval shown in Fig.1, and x is the displacement in the $\hat{x} = (1,0)$ direction.

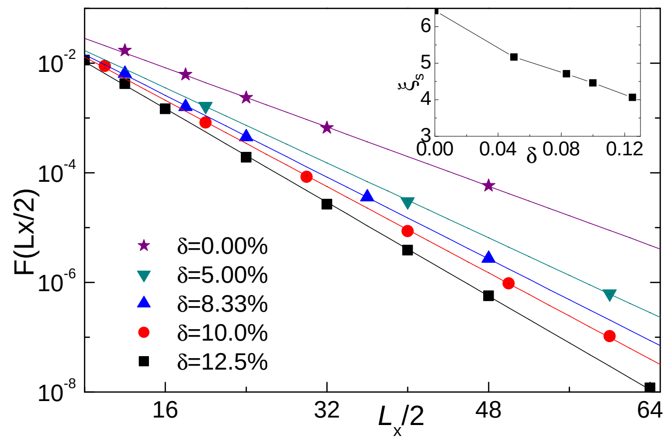

FIG. 4: (Color online) Finite-size scaling of the spin-spin correlation $F(\frac{L_x}{2})$ as a function of L_x at $\delta = 0\%$ to 12.5% in the semi-logarithemic plot. The inset shows the correlation length ξ_s obtained from fits (solid lines) to data in the main panel using $F(\frac{L_x}{2}) \propto e^{-L_x/2\xi_s}$.

Fig.2 shows the finite-size scaling of $\Phi_{yy}(\frac{L_x}{2})$ at different doping levels. It decays with a power-law, whose exponent K_{sc}, plotted in Fig.3, was obtained by fitting the results using Eq.(2). Therefore, we can conclude that the lightly doped t-J model on $L_y = 4$ cylinders has quasi-long-range SC correlation. It is worth noting that K_{sc} decreases with decreasing δ tending to saturate at $K_{sc} = 0.5$, while K_c increases and tends to saturate at $K_c = 2$ as $\delta \to 0$. Both tendencies are consistent with theoretical prediction.[25]

Spin-spin correlation: To describe the magnetic properties of the ground state, we have also calculated the spin-spin correlation functions defined as

$$F(x) = \frac{1}{L_y}\sum_{y=1}^{L_y} |\langle \vec{S}_{x_0,y} \cdot \vec{S}_{x_0+x,y}\rangle|. \tag{4}$$

Here $\vec{S}_{x,y}$ denotes the spin operator on site $i = (x,y)$. (x_0, y) is the reference site indicated by the red oval shown in Fig.1, and x is the displacement in the $\hat{x} = (1,0)$ direction. As we did for A_{cdw} and Φ_{yy}, we first extrapolate $F(\frac{L_x}{2})$ to the limit $m = \infty$, and then analyze the functional dependence of the result on L_x. As shown in Fig.4, $F(\frac{L_x}{2})$ decays exponentially with L_x, i.e., $F(\frac{L_x}{2}) \propto e^{-L_x/2\xi_s}$. The corresponding correlation length is $\xi_s = 4 \sim 5$ lattice spacings. We conclude that the spin correlations are short-ranged and consequently that there is a spin-gap.

Anti-periodic boundary condition: We have also considered cylinders with anti-periodic boundary condition (ABC) in the $\hat{y}$ direction in order to test the extent to which our results are representative of the 2D limit. As shown in Fig.5 and previous studies[16], the influence of changing boundary condition around the cylinder is significant. For example, the ground state of short cylinders with length $L_x \leq 48$, e.g., the $L_x = 32$ cylinder in

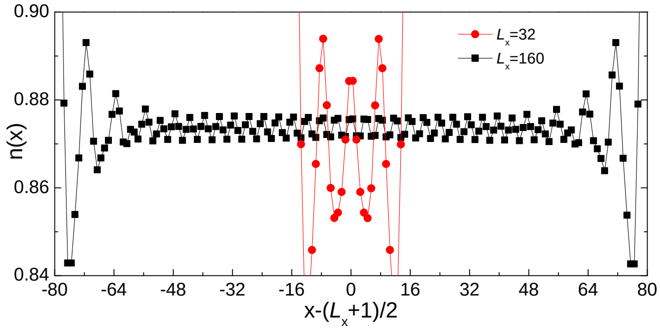

FIG. 5: (Color online) The charge density profile $n(x)$ at $\delta = 12.5\%$ and ABC in the $\hat{y}$ direction for $L_x = 32$ and $L_x = 160$ cylinders.

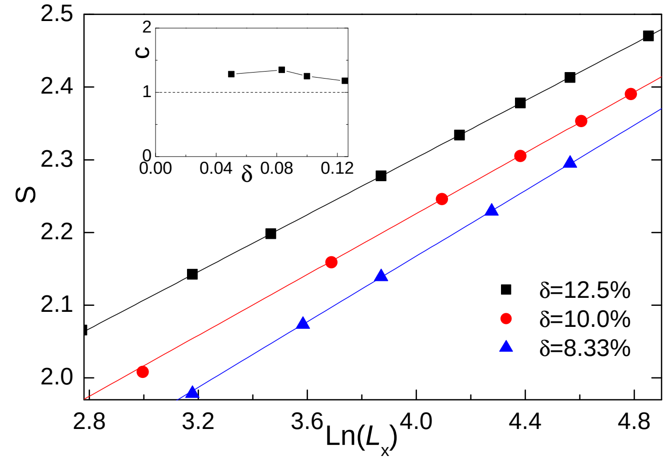

FIG. 6: (Color online) Von Neumann entanglement entropy S with $\delta = 8.33\%$, 10% and 12.5%. Inset: The extracted central charge c as a function of δ. Dashed line marks $c = 1$.

Fig.5, forms charge stripes of wavelength $\lambda = \frac{1}{\delta}$, which are completely filled with holes. However, this turns out to be a finite-size effect; the bulk of longer cylinders with length $L_x \geq 64$ exhibits half-filled stripes with wavelength $\lambda = 1/2\delta$, which is the same as the charge stripes of cylinders with periodic boundary conditions. Examples of the charge density distribution of cylinders with ABC in the $\hat{y}$ direction are given in Fig.5 for $\delta = 12.5\%$. The ABC apparently affects the balance between filled and half-filled charge stripes; the former are stabilized in a finite region close to the open boundaries of the cylinder, while half-filled stripes are robust in the bulk.

Central charge: A key feature of the LE liquid is that it has a single gapless mode, i.e. it is expected to exhibit central charge $c = 1$. The central charge can be obtained by calculating the von Neumann entropy $S = -\mathrm{Tr}\rho\ln\rho$, where ρ is the reduced density matrix of a subsystem with length l. For critical systems in 1+1 dimensions, it has been established[26] that $S(l) = \frac{c}{6}\ln(l) + \tilde{c}$ for open systems, where c is the central charge of the CFT and $\tilde{c}$ denotes a model dependent constant. For finite cylinders with length L_x, we can fix $l = \frac{L_x}{2}$ to extract the central charge c. Fig.6 shows $S(\frac{L_x}{2})$ at different doping levels δ. The inset shows the fitted central charge c as a function of δ. Although the extracted value of central charge c is slightly larger than $c = 1$, we suspect that this is within the uncertainty of the calculation. The result is roughly consistent with one gapless charge mode with $c = 1$, which thus provides additional evidence for the presence of a LE liquid in the doped t-J model.

Summary and Discussion: The presence of power-law superconducting correlations with $K_{sc} < 2$ on 4-leg cylinders is an encouraging piece of evidence of the possible existence of a high temperature superconducting phase in 2D. The $Q = 4\pi\delta$ CDW correlations are reminiscent of the experimentally observed "half-filled" CDW order that has been observed in previous DMRG studies of t-J models,[12] in DQMC studies of the Hubbard model at elevated temperatures,[17,18] and experimentally in several cuprates. The spin correlation length (shown in Fig.4) decreases monotonically with increasing δ from $\xi_s \simeq 6.5$ for $\delta = 0$ to $\xi_s \simeq 4$ for $\delta = 12.5\%$.

It is still unclear how the interplay between SC and CDW order should be expected to evolve with increasing cylinder circumference L_y. This uncertainty is exacerbated by the large number of nearly degenerate ground-state phases that were found previously[16] to be stabilized by relatively small changes in the microscopic parameters of the model. The subtlety of the interplay between multiple phases is illustrated by changing the boundary conditions on the electronic wave-functions from periodic to anti-periodic. As shown in Fig.5, on shorter cylinders (e.g. $L_x = 32$), a distinct CDW state with $Q = 2\pi\delta$ is stabilized. This state is reminiscent of the "filled" stripes found in Hartree-Fock calculations[27–29] (where it is accompanied by long-range SDW order) and using various approximate methods[14] used in studies of the 2D Hubbard model.[33] In the present case, we find that while even for much longer flux-pierced cylinders, while the filled stripe state is observable locally for a finite region near the ends of the cylinders, far from the ends the CDW correlations have the same $Q = 4\pi\delta$ ordering vector as in the fluxless cylinder.

One big question is the fate of the magnetic correlations in the 2D limit. For $\delta = 0$, on theoretical grounds[30,31] we know that ξ_s should diverge with $L_y \to \infty$ since the ground-state of the spin-1/2 Heisenberg model is magnetically ordered in 2D. The shorter correlation lengths of the doped systems suggests, but does not establish, that long-range antiferromagnetic order is unlikely to persist in 2D for even relatively modest values of δ.

Acknowledgement: We would like to thank T. Devereaux, D. J. Scalapino, J. Tranquada, J. Zaanen, A. Broido, Y. F. Jiang and J. Dodaro for insightful discussions. This work was supported by the Department of Energy, Office of Science, Basic Energy Sciences, Materials Sciences and Engineering Division, under Contract DE-AC02-76SF00515.

* Electronic address: hcjiang@stanford.edu

[1] Editorial, The hubbard model at half a century, Nature Physics 9, 523 (2013).
[2] T. Giamarchi, Quantum physics: A firmer grip on the hubbard model, Nature 545, 414 (2017).
[3] E. Dagotto, J. Riera, and D. Scalapino, Superconductivity in ladders and coupled planes, Phys. Rev. B 45, 5744 (1992).
[4] H. Tsunetsugu, M. Troyer, and T. M. Rice, Pairing and excitation spectrum in doped t-J ladders, Phys. Rev. B 49, 16078 (1994).
[5] M. Troyer, H. Tsunetsugu, and T. M. Rice, Properties of lightly doped t-J two-leg ladders, Phys. Rev. B 53, 251 (1996).
[6] E. Arrigoni, E. Fradkin, and S. A. Kivelson, Mechanism of high-temperature superconductivity in a striped Hubbard model, Phys. Rev. B 69, 214519 (2004).
[7] G. Hager, G. Wellein, E. Jeckelmann, and H. Fehske, Stripe formation in doped Hubbard ladders, Phys. Rev. B 71, 075108 (2005).
[8] Z. Zhu, H. C. Jiang, D. N. Sheng, and Z. Y. Weng, Nature of strong hole pairing in doped mott antiferromagnets, Scientific Reports 4, 5419 (2014).
[9] M.-S. Chang and I. Affleck, Bipairing and the stripe phase in four-leg Hubbard ladders, Phys. Rev. B 76, 054521 (2007).
[10] M. Machida, S. Yamada, M. Okumura, Y. Ohashi, and H. Matsumoto, Stripe formation in repulsive 4-leg Hubbard ladder: Directly-extended dmrg studies, Physica C-Superconductivity and its Application, 468, 1141 (2007).
[11] M. Dolfi, B. Bauer, S. Keller, and M. Troyer, Pair correlations in doped Hubbard ladders, Phys. Rev. B 92, 195139 (2015).
[12] S. R. White and D. J. Scalapino, Ground states of the doped four-leg t-J ladder, Phys. Rev. B 55, R14701 (1997).
[13] S. Liu, H.-C. Jiang, and T. P. Devereaux, Nature of a single doped hole in two-leg Hubbard and t-J ladders, Phys. Rev. B 94, 155149 (2016).
[14] B.-X. Zheng, C.-M. Chung, P. Corboz, G. Ehlers, M.-P. Qin, R. M. Noack, H. Shi, S. R. White, S. Zhang, and G. K.-L. Chan, Stripe order in the underdoped region of the two-dimensional Hubbard model, Science 358, 1155 (2017).
[15] Y.-F. Jiang, H.-C. Jiang, H. Yao, and S. A. Kivelson, Fractional charge and emergent mass hierarchy in diagonal two-leg t-J cylinders, Phys. Rev. B 95, 245105 (2017).
[16] J. F. Dodaro, H.-C. Jiang, and S. A. Kivelson, Intertwined order in a frustrated four-leg t-J cylinder, Phys. Rev. B 95, 155116 (2017).
[17] E. W. Huang, C. B. Mendl, S. Liu, S. Johnston, H.-C. Jiang, B. Moritz, and T. P. Devereaux, Numerical evidence of fluctuating stripes in the normal state of high-t_c cuprate superconductors, Science 358, 1161 (2017).
[18] E. W. Huang, C. B. Mendl, H. C. Jiang, B. Moritz, and T. P. Devereaux, Stripe order from the perspective of the Hubbard model, NPJ Quantum Materials 3, 22 (2018).
[19] E. Dagotto, Correlated electrons in high-temperature superconductors, Rev. Mod. Phys. 66, 763 (1994).
[20] P. A. Lee, N. Nagaosa, and X.-G. Wen, Doping a mott insulator: Physics of high-temperature superconductivity, Rev. Mod. Phys. 78, 17 (2006).
[21] S. R. White, Density matrix formulation for quantum renormalization groups, Phys. Rev. Lett. 69, 2863 (1992).
[22] A. Luther and V. J. Emery, Backward scattering in the one-dimensional electron gas, Phys. Rev. Lett. 33, 589 (1974).
[23] H. C. Jiang and T. P. Devereaux, Superconductivity in the doped Hubbard model: interplay with doped charged stripes and next nearest hopping t', arXiv:1806.01465 (2018).
[24] T. Siller, M. Troyer, T. M. Rice, and S. R. White, Transition between hole pairs and four-hole clusters in four-leg t-J ladders, Phys. Rev. B 65, 205109 (2002).
[25] L. Balents and M. P. A. Fisher, Weak-coupling phase diagram of the two-chain Hubbard model, Phys. Rev. B 53, 12133 (1996).
[26] P. Calabrese and J. Cardy, Entanglement entropy and quantum field theory, Journal of Statistical Mechanics: Theory and Experiment 2004, P06002 (2004).
[27] J. Zaanen and O. Gunnarsson, Charged magnetic domain lines and the magnetism of high-T_c oxides, Phys. Rev. B 40, 7391 (1989).
[28] K. Machida, Magnetism in La_2CuO_4 based compounds, Physica C Superconductivity 158, 192 (1989).
[29] H. J. Schulz, Incommensurate antiferromagnetism in the two-dimensional Hubbard model, Phys. Rev. Lett. 64, 1445 (1990).
[30] S. Chakravarty, Dimensional Crossover in Quantum Antiferromagnets, Phys. Rev. Lett. 77, 4446 (1996).
[31] O. F. Syljuåsen, S. Chakravarty, and M. Greven, Correlation Lengths in Quantum Spin Ladders, Phys. Rev. Lett. 78, 4115 (1997).
[32] See Supplemental Material at [URL] for more details.
[33] Such a state was also found for 4-leg cylinders with $t' \approx 0.06-0.08t$ in Ref.16.